HHS Public Access

Author manuscript

Nat Neurosci. Author manuscript; available in PMC 2016 May 18.

Published in final edited form as:

Nat Neurosci. 2015 December ; 18(12): 1722–1724. doi:10.1038/nn.4159.

Latent tri-lineage potential of adult hippocampal neural stem cells revealed by *Nf1* inactivation

Gerald J. Sun[1,2], **Yi Zhou**[1,3], **Shiori Ito**[1], **Michael A. Bonaguidi**[1,4], **Genevieve Stein-O'Brien**[5], **Nicholas Kawasaki**[1], **Nikhil Modak**[1], **Yuan Zhu**[6], **Guo-li Ming**[1,2,3,4,7,*], and **Hongjun Song**[1,2,3,4,5,*]

[1]Institute for Cell Engineering, Johns Hopkins University School of Medicine, Baltimore, MD 21205, USA

[2]The Solomon H. Snyder Department of Neuroscience, Johns Hopkins University School of Medicine, Baltimore, MD 21205, USA

[3]The Biochemistry, Cellular and Molecular Biology Graduate Program, Johns Hopkins University School of Medicine, Baltimore, MD 21205, USA

[4]Department of Neurology, Johns Hopkins University School of Medicine, Baltimore, MD 21205, USA

[5]Pre-doctoral Human Genetics Training Program, Johns Hopkins University School of Medicine, Baltimore, MD 21205, USA

[6]Gilbert Family Neurofibromatosis Institute, Center for Cancer and Immunology Research, Children's National Medical Center, Washington, DC 20010, USA

[7]Department of Psychiatry and Behavioral Sciences, Johns Hopkins University School of Medicine, Baltimore, MD 21205, USA

Abstract

Endogenous neural stem cells (NSCs) in the adult hippocampus are considered bi-potent, as they only produce neurons and astrocytes *in vivo*. Here we show in mouse that inactivation of neurofibromin 1, a gene mutated in neurofibromatosis type 1, unlocks a latent oligodendrocyte lineage potential to produce all three lineages from NSCs *in vivo*. Our results suggest an avenue to promote stem cell plasticity by targeting barriers of latent lineage potential.

It had been long postulated that continuous neurogenesis in restricted regions of the adult mammalian brain originates from tri-potent NSCs[1]. Early supporting evidence includes *in vivo* observations of new neurons, astrocytes and oligodendrocytes in the subventricular

*Correspondence should be addressed to: Hongjun Song, Ph.D. (; Email: shongju1@jhmi.edu), Guo-li Ming, M.D. & Ph.D. (; Email: gming1@jhmi.edu)

AUTHOR CONTRIBUTIONS: G.J.S., H.S., and G.M. deigned the project. G.J.S. contributed to all aspects of the study; Y. Zhou, S.I., G.S-O., N.K. and N.M. performed experiments; M.A.B. provided some initial data; Y. Zhu contributed reagents; G.J.S., H.S., and G.M. wrote the manuscript.

COMPETING FINANCIAL INTERESTS: The authors declare no competing financial interests.

zone (SVZ) of lateral ventricles and hippocampal dentate gyrus, and *in vitro* demonstrations of tri-potency of individual adult NSCs upon derivation and expansion[2]. However, recent population fate-mapping and clonal lineage-tracing of NSCs in the adult hippocampus have consistently found generation of neurons and astrocytes, but not oligodendrocytes. In the adult SVZ, population fate-mapping studies have shown generation of both neurons and oligodendrocytes[3], but *in vivo* clonal analysis found only neuronal lineages[4] and *in vitro* time-lapse analysis revealed that individual acutely isolated NPCs generate either neurons, or oligodendrocytes, but never both[5]. Therefore, whether NSCs with an intrinsic tri-lineage potential exist in the adult mammalian brain remains a fundamental question. How endogenous NSC lineage potential is regulated is also unknown. Incidentally, we discovered that conditional inactivation of neurofibromin 1 (*Nf1*) in normally bi-potent radial glia-like NSCs (RGLs) in the adult dentate gyrus unlocks their latent oligodendrocytic lineage potential *in vivo*.

Mutations of *Nf1* cause neurofibromatosis type 1, a disease characterized by increased risk of nervous system tumorigenesis and manifestation of specific learning disabilities[6]. NF1 regulates progenitor proliferation and fate specification[6], yet its role in NSCs in the adult hippocampus – a region critical for learning and memory, remains largely unknown. We utilized a tamoxifen-inducible *Nestin*^{CreERT2} mouse line containing floxed *Nf1* exons 31 and 32 and a Z/EG reporter (*Nestin*^{CreERT2}*;Nf1*$^{f/f}$*;Z/EG*) with multiple tamoxifen injections (Supplementary Fig. 1a–b), a paradigm previously used to conditionally inactivate *Nf1* and identify deficits in progenitor proliferation and new neuron development in the adult hippocampus[7]. Total numbers of labeled neurons observed 1 month post-tamoxifen injection (mpi) in *Nestin*^{CreERT2}*;Nf1*$^{f/f}$*;Z/EG* (Nf1^{Nestin}) were comparable to those in *Nestin*^{CreERT2}*;Z/EG* (control^{Nestin}) animals (Fig. 1a–b). Surprisingly, in Nf1^{Nestin} animals, a large number of GFP^{+} cells exhibited oligodendrocyte progenitor cell (OPC) morphology and expressed NG2, but not GFAP (Fig. 1c). The presence of GFP^{+}NG2^{+}MCM2^{+} cells indicated that active proliferation of RGL-derived OPCs contributed to their final production (Supplementary Fig. 1c). Consistent with previous studies[8–12], OPCs were never observed in control^{Nestin} animals (n = 3,564 cells) or *Nestin*^{CreERT2}*;Nf1*$^{f/+}$*;Z/EG* animals (n = 2,568 cells; Supplementary Table 1), suggesting requirement of biallelic *Nf1* inactivation for OPC production. Interestingly, at 14 days post-tamoxifen injection (dpi), Olig2 was expressed in 10 ± 3% (mean ± s.d.) GFP^{+} RGLs in Nf1^{Nestin}, but none in control^{Nestin} animals (n = 3 animals for each condition; Supplementary Fig. 1d), suggesting a potential molecular mechanism. Similar ectopic Olig2 expression was found in the adult SVZ upon *Nf1* inactivation, which also leads to increased OPC production[13]. No difference in the percentage of MCM2^{+} RGLs upon *Nf1* inactivation was found at 2 or 14 dpi (n = 3 hemispheres for each condition; $p \geq 0.4$; two-tailed unpaired t-test).

Both *Nf1* inactivation in OPCs and stress are known to induce OPC proliferation *in vivo*[14,15]. To rule out the possibility that rare OPCs were initially labeled and became amplified, we examined Nf1^{Nestin} and control^{Nestin} animals at 2 dpi. No GFP^{+} OPCs were observed across the hippocampus (Fig. 1d, e; control^{Nestin}: n = 1,734 cells; Nf1^{Nestin}: n = 669 cells; Supplementary Table 1). Together, these data showed *de novo* generation of the OPC lineage from adult NSCs that normally give rise to only neurons and astrocytes *in vivo*.

To ascertain the origin of new OPCs upon *Nf1* inactivation and assess properties of individual NSCs, we performed clonal lineage-tracing of RGLs in the adult dentate gyrus (Supplementary Fig. 2a). Utilizing a single low-dose tamoxifen injection in $Nf1^{Nestin}$ or $control^{Nestin}$ mice, we sparsely labeled on average 10 ± 1 precursors, including RGLs and very few intermediate neural progenitors, across the entire dentate gyrus at 2 dpi (n = 8 animals). No GFP^+ OPCs were observed in any clones at 2 dpi ($Nf1^{Nestin}$: 0/71 clones; $control^{Nestin}$: 0/50 clones; Supplementary Table 2). At 1 or 2 mpi, we observed $Nf1^{Nestin}$ clones that contained $NG2^+$ cells with OPC morphology (6/142; Fig. 2a–b). Some clones contained astrocytes, OPCs and an RGL in close proximity (Fig. 2a; Movie S1); other clones lacked RGLs, potentially due to RGL differentiation[10] or death (Fig. 2b). Consistent with our previous characterizations of RGLs in multiple clonal lineage-tracing studies[10–12] (over 504 clones in total), no OPCs were present in any $control^{Nestin}$ clones in the current study (0/82; Supplementary Table 2). Some RGLs with four rounds of cell division still did not generate OPCs in $control^{Nestin}$ animals (Fig. 2c). Most $Nf1^{Nestin}$ clones (136/142) did not produce OPCs (Fig. 2d), which could have been due to incomplete recombination of both reporter and *Nf1* floxed alleles in the same cell upon a single low-dose tamoxifen induction, and/or *Nf1* inactivation only unlocks the potential for, but does not restrict the RGL fate to OPCs as shown in population fate mapping (Fig. 1). Notably, the size of $Nf1^{Nestin}$ clones with OPCs was larger than those of $control^{Nestin}$ at 1 mpi (Supplementary Fig. 2b). Consistent with a previous report[7], some $Nf1^{Nestin}$ clones at 1 or 2 mpi contained mis-positioned labeled neurons, indicative of successful Nf1 inactivation in at least some of labeled clones. Strikingly, some neurons in $Nf1^{Nestin}$ clones migrated into the molecular layer (Supplementary Fig. 2c), suggesting a critical role of NF1 in regulating migration of newborn neurons during adult neurogenesis.

We validated our finding by clonal analysis using an independent tamoxifen-inducible $Gli1^{CreERT2}$ line that also specifically targets RGLs in the adult dentate gyrus[16]. We generated two mouse lines: $Gli1^{CreERT2};Nf1^{f/f};Z/EG$ ($Nf1^{Gli1}$) and $Gli1^{CreERT2};Z/EG$ ($control^{Gli1}$; Supplementary Fig. 3a). No GFP^+ OPCs were observed at 2 dpi ($Nf1^{Gli1}$: 0/20 clones; $control^{Gli1}$: 0/34 clones; Supplementary Table 3). At 1 mpi, we observed OPC-containing clones in $Nf1^{Gli1}$ animals (8/64 clones), but never in $control^{Gli1}$ animals (0/38 clones; Supplementary Fig. 2b–c; Supplementary Table 3). Strikingly, some clones at 1 mpi in $Nf1^{Gli1}$ animals contained three lineages: neurons, astrocytes, and OPCs (3/64 clones; Supplementary Fig. 3b). Together, these results suggest that RGLs in the adult hippocampus possess an intrinsic ability to generate all three major neural lineages, and the OPC lineage potential is actively restricted by NF1.

The concept of adult NSCs with a defining trait of multi-lineage neuronal, astrocytic and oligodendrocytic potential was established over two decades ago[1], yet no endogenous tri-potent NSCs have been shown. In the current model, NSCs are gradually specified during development and become restricted in their lineage potential in adult[17]; they can only regain the tri-potentiality *in vitro* upon removal from their local environment and treatment with growth factors. Our results suggest a new model whereby adult NSCs are intrinsically tri-potent and their fate specification is regulated not only by positive instructive cues, but also by inhibitory signaling that actively suppresses certain fates (Supplementary Fig. 4). Since NF1, a cytoplasmic regulator of Ras and cAMP signaling[6], is neither a transcription factor,

nor a known direct reprogramming factor, our model is conceptually different from reprogramming, for example, in the case of a neuronal to oligodendrocytic fate switch upon forced *Ascl1* overexpression in proliferating hippocampal neural progenitors[18]. *Nf1* inactivation does not convert RGLs to OPCs, as other fates are still produced. Instead, our result supports an emerging view that latent lineage potentials could be actively suppressed in precursors or even in apparently differentiated cell types. For example, adult striatal astrocytes were recently shown to exhibit a latent neurogenic program that is actively suppressed by Notch signaling[19] and can be elicited by injury[20]. This new framework enriches our understanding of fundamental stem cell biology and opens new avenues for stem cell plasticity or therapeutics via targeting barriers of a cell's intrinsic lineage potential.

ONLINE METHODS

Animals and tamoxifen administration

Nestin^{CreERT2};*Nf1*$^{f/f}$;*Z/EG*$^{f/-}$, *Nestin*^{CreERT2};*Nf1*$^{f/+}$;*Z/EG*$^{f/-}$, and *Nestin*^{CreERT2};*Z/EG*$^{f/-}$ mice were generated by crossing *Nestin*^{CreERT2} driver[21] with *Z/EG*$^{f/-}$ reporter[22] (Tg(CAG-Bgeo/GFP)21Lbe/J, Jackson Labs) and *Nf1*$^{f/f}$ mice[23], where applicable. *Gli1*^{CreERT2};*Nf1*$^{f/f}$;*Z/EG*$^{f/-}$ and *Gli1*^{CreERT2};*Z/EG*$^{f/-}$ mice were generated in a similar fashion, but with *Gli1*^{CreERT2} mice[16]. All mice in the study were backcrossed to the C57BL/6 background for at least six generations. Animals were housed in a 14 hour light/10 hour dark cycle and had free access to food and water. Tamoxifen (66.67 mg/ml, Sigma, T5648) was prepared in a 5:1 corn oil (Sigma) to ethanol mixture. Due to differences in CreER^{T2} mouse generation, different tamoxifen injection paradigms were required to enable sparse labeling for clonal analysis (~ 8–16 clones per hemisphere). A single 62.5 mg/kg dose of tamoxifen (for *Nestin*^{CreERT2}) or a 125 mg/kg dose every 12 hours for 4 total doses (for *Gli1*^{CreERT2}) was intraperitoneally injected into adult 8–10 week-old male and female mice (Supplementary Table 4). For population cell labeling in *Nestin*^{CreERT2}, animals were injected with 125 mg/kg every 12 hours 4 times (Supplementary Table 4). Animals were analyzed at 2 dpi, 14 dpi, or 1–2 mpi. For animals with multiple injections, dpi and mpi were counted starting from the final injection. All animal procedures were performed in accordance to institutional guidelines of Johns Hopkins University School of Medicine.

Tissue processing, immunostaining and confocal imaging

Animals were transcardiac perfused with cold 4% paraformaldehyde (wt/vol, in 0.1 M phosphate buffer, PB, pH 7.4), and cryoprotected with 30% sucrose (wt/vol). Serial 40 μm-thick coronal brain sections were cut on a frozen sliding microtome (Leica, SM2010R) for immunohistology as previously described[10,24]. Antibodies diluted in TBS with 0.05% Triton X-100 and 3% donkey serum, were used against GFP (Aves Labs, GFP-1020, chicken, 1:500; Rockland, 600-101-215, goat, 1:500; AbD Serotec, 4745-1051, sheep, 1:500), Tbr2 (Abcam, ab23345, rabbit, 1:250), GFAP (Millipore, MAB360, mouse, 1:1000; DAKO, Z033401-2, rabbit, 1:1000), Nestin (Aves Labs, NES, chicken, 1:500), Prox1 (Millipore, MAB5654, mouse, 1:500), NG2 (Millipore, AB5320, rabbit, 1:200), Olig2 (a generous gift from Dr. Bennett Novitch, guinea pig, 1:20000). Nestin antigen was retrieved by incubating brain sections in 1X DAKO target retrieval solution (DAKO) at 68°C for 20 minutes, followed by 10 minutes cooling to room temperature. Serial sections from the entire dentate

gyrus were first immunostained for GFP to allow identification of prospective clone-containing sections on an epifluorescence microscope (Zeiss, Axiovert 200M). Labeled clone-containing sections were taken for further processing and confocal imaging at 40X on a Zeiss LSM 710 confocal microscope using multi-track or spectral linear unmixing 'online fingerprinting' configurations (Carl Zeiss).

Image processing and data analyses

For population cell labeling experiments, cells were counted manually by visualizing the serial dentate gyrus sections on an epifluorescence microscope. Due to the difficulty in reliably quantifying small, densely packed transient-amplifying neural progenitors, only cells with mature neuron morphology were counted as belonging to the neuronal lineage at 1 mpi. For clonal cell labeling experiments, identification of clones amongst GFP-labeled clusters of cells was performed as previously described[10,25]. Clones that spanned multiple serial sections were reconstructed using Reconstruct software as previously described[10,25]. All aligned images were exported at full resolution for 3D visualization into Imaris (Bitplane) and analyzed. All other confocal images were directly visualized and analyzed in Imaris. Movie of 3D-rendered clone was generated using the Animation feature in Imaris. Clones were analyzed in a dentate gyrus volume that included the molecular layer, granule cell layer, subgranular zone, and hilus, excluding the polymorphic layer (CA4) protruding into the posterior dentate gyrus. Clonal cell fate frequencies were calculated per brain hemisphere and averaged across hemispheres. Numbers of cells and animals counted and used, respectively, are shown in Supplementary Tables 1–3. No statistical methods were used to pre-determine sample sizes; sample sizes were similar to those reported in previous studies[10,11] Due to the binary nature of the reported phenomenon, randomization and blinding were not employed. A two-sample Kolmogorov–Smirnov test was used to statistically compare clone cell number distributions. A two-sample unpaired Student's t-test was used to statistically compare the percentage of $MCM2^+$ RGLs upon *Nf1* inactivation at 2 or 14 dpi.

Supplementary Material

Refer to Web version on PubMed Central for supplementary material.

ACKNOWLEDGMENTS

We thank members of Ming and Song laboratories for discussion, Y. Cai and L. Liu for technical support. This work was supported by NIH (NS047344 to H.S., NS080913 to M.A.B., and NS048271 and MH105128 to G.M.), and by a pre-doctoral fellowship from The Children's Tumor Foundation to G.J.S.

REFERENCES

1. Gage FH. Mammalian neural stem cells. Science. 2000; 287:1433–1438. [PubMed: 10688783]
2. Ming GL, Song H. Adult neurogenesis in the mammalian brain: significant answers and significant questions. Neuron. 2011; 70:687–702. [PubMed: 21609825]
3. Menn B, et al. Origin of oligodendrocytes in the subventricular zone of the adult brain. J Neurosci. 2006; 26:7907–7918. [PubMed: 16870736]
4. Calzolari F, et al. Fast clonal expansion and limited neural stem cell self-renewal in the adult subependymal zone. Nat Neurosci. 2015; 18:490–492. [PubMed: 25730673]

5. Ortega F, et al. Oligodendrogliogenic and neurogenic adult subependymal zone neural stem cells constitute distinct lineages and exhibit differential responsiveness to Wnt signalling. Nature cell biology. 2013; 15:602–613. [PubMed: 23644466]
6. Gutmann DH, Parada LF, Silva AJ, Ratner N. Neurofibromatosis type 1: modeling CNS dysfunction. The Journal of neuroscience : the official journal of the Society for Neuroscience. 2012; 32:14087–14093. [PubMed: 23055477]
7. Li Y, Li Y, McKay RM, Riethmacher D, Parada LF. Neurofibromin modulates adult hippocampal neurogenesis and behavioral effects of antidepressants. J Neurosci. 2012; 32:3529–3539. [PubMed: 22399775]
8. Lagace DC, et al. Dynamic contribution of nestin-expressing stem cells to adult neurogenesis. J Neurosci. 2007; 27:12623–12629. [PubMed: 18003841]
9. Dranovsky A, et al. Experience dictates stem cell fate in the adult hippocampus. Neuron. 2011; 70:908–923. [PubMed: 21658584]
10. Bonaguidi MA, et al. In vivo clonal analysis reveals self-renewing and multipotent adult neural stem cell characteristics. Cell. 2011; 145:1142–1155. [PubMed: 21664664]
11. Song J, et al. Neuronal circuitry mechanism regulating adult quiescent neural stem-cell fate decision. Nature. 2012; 489:150–154. [PubMed: 22842902]
12. Jang MH, et al. Secreted frizzled-related protein 3 regulates activity-dependent adult hippocampal neurogenesis. Cell Stem Cell. 2013; 12:215–223. [PubMed: 23395446]
13. Wang Y, et al. ERK inhibition rescues defects in fate specification of Nf1-deficient neural progenitors and brain abnormalities. Cell. 2012; 150:816–830. [PubMed: 22901811]
14. Liu C, et al. Mosaic analysis with double markers reveals tumor cell of origin in glioma. Cell. 2011; 146:209–221. [PubMed: 21737130]
15. Chetty S, et al. Stress and glucocorticoids promote oligodendrogenesis in the adult hippocampus. Molecular psychiatry. 2014; 19:1275–1283. [PubMed: 24514565]
16. Ahn S, Joyner AL. In vivo analysis of quiescent adult neural stem cells responding to Sonic hedgehog. Nature. 2005; 437:894–897. [PubMed: 16208373]
17. Kriegstein A, Alvarez-Buylla A. The glial nature of embryonic and adult neural stem cells. Annual review of neuroscience. 2009; 32:149–184.
18. Jessberger S, Toni N, Clemenson GD Jr, Ray J, Gage FH. Directed differentiation of hippocampal stem/progenitor cells in the adult brain. Nat Neurosci. 2008; 11:888–893. [PubMed: 18587391]
19. Magnusson JP, et al. A latent neurogenic program in astrocytes regulated by Notch signaling in the mouse. Science. 2014; 346:237–241. [PubMed: 25301628]
20. Nato G, et al. Striatal astrocytes produce neuroblasts in an excitotoxic model of Huntington's disease. Development. 2015; 142:840–845. [PubMed: 25655705]
21. Balordi F, Fishell G. Mosaic removal of hedgehog signaling in the adult SVZ reveals that the residual wild-type stem cells have a limited capacity for self-renewal. J Neurosci. 2007; 27:14248–14259. [PubMed: 18160632]
22. Novak A, Guo C, Yang W, Nagy A, Lobe CG. Z/EG, a double reporter mouse line that expresses enhanced green fluorescent protein upon Cre-mediated excision. Genesis. 2000; 28:147–155. [PubMed: 11105057]
23. Zhu Y, et al. Ablation of NF1 function in neurons induces abnormal development of cerebral cortex and reactive gliosis in the brain. Genes Dev. 2001; 15:859–876. [PubMed: 11297510]
24. Berg DK, et al. Tbr2-expressing intermediate progenitor cells in the adult mouse hippocampus are unipotent neuronal precursors with limited amplification capacity under homeostasis. Front Biol (Beijing). 2015; 10:262–271.
25. Sun GJ, et al. Tangential migration of neuronal precursors of glutamatergic neurons in the adult mammalian brain. Proc Natl Acad Sci U S A. 2015

Additional References

21. Balordi F, Fishell G. Mosaic removal of hedgehog signaling in the adult SVZ reveals that the residual wild-type stem cells have a limited capacity for self-renewal. J Neurosci. 2007; 27:14248–14259. [PubMed: 18160632]
22. Novak A, Guo C, Yang W, Nagy A, Lobe CG. Z/EG, a double reporter mouse line that expresses enhanced green fluorescent protein upon Cre-mediated excision. Genesis. 2000; 28:147–155. [PubMed: 11105057]
23. Zhu Y, et al. Ablation of NF1 function in neurons induces abnormal development of cerebral cortex and reactive gliosis in the brain. Genes Dev. 2001; 15:859–876. [PubMed: 11297510]
24. Berg DK, et al. Tbr2-expressing intermediate progenitor cells in the adult mouse hippocampus are unipotent neuronal precursors with limited amplification capacity under homeostasis. Front Biol (Beijing). 2015; 10:262–271.
25. Sun GJ, et al. Tangential migration of neuronal precursors of glutamatergic neurons in the adult mammalian brain. Proc Natl Acad Sci U S A. 2015

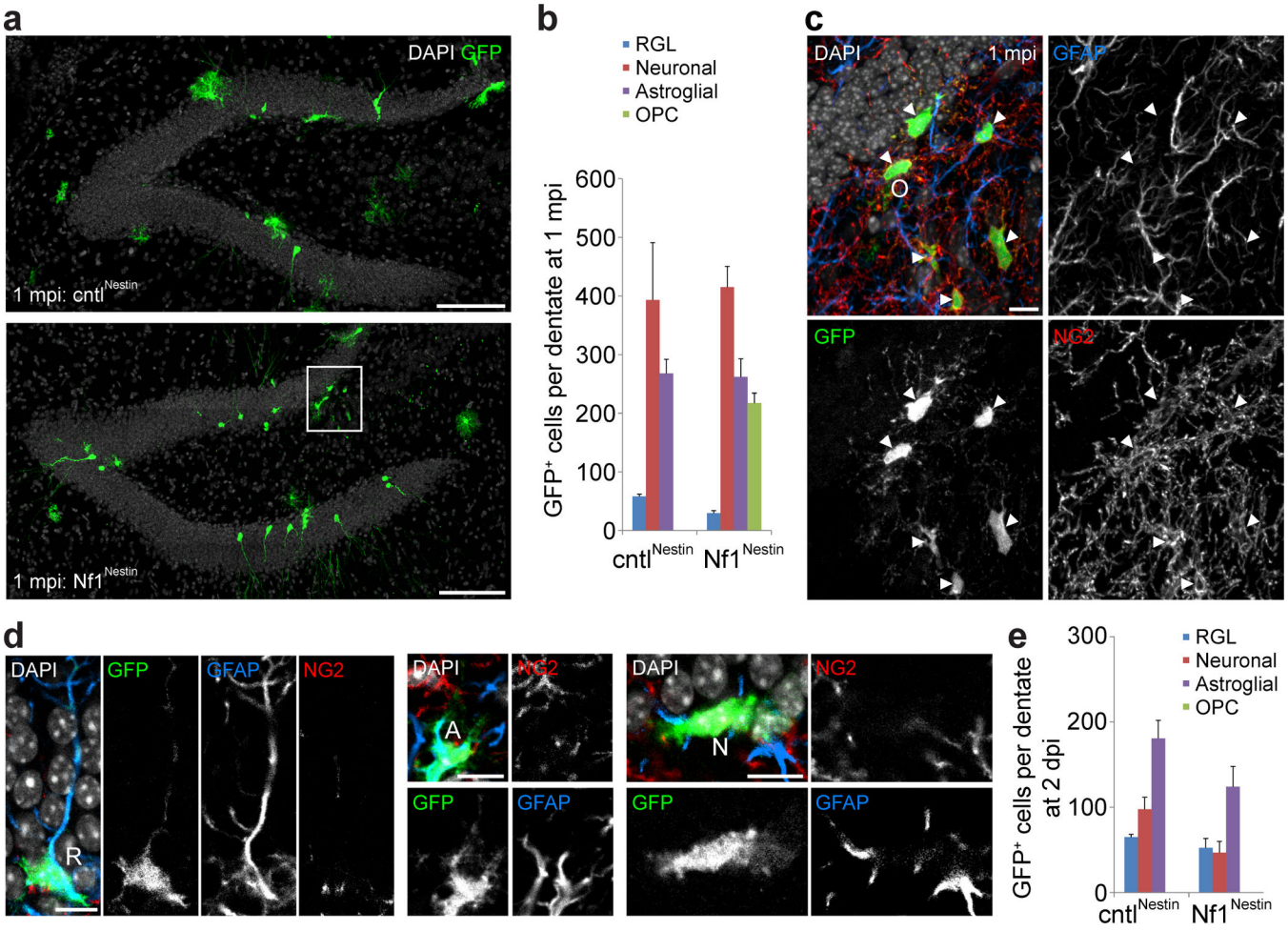

Figure 1.

Nestin^{CreERT2}-based conditional *Nf1* inactivation in adult hippocampal neural progenitors leads to generation of oligodendrocyte progenitor cells. **(a)** Sample projected confocal images in the population-labeling paradigm at 1 mpi in control^{Nestin} (top) and Nf1^{Nestin} (bottom) animals. **(b)** Quantification of total GFP^{+} cell numbers by lineage across the dentate gyrus at 1 mpi. Values represent mean ± s.e.m. **(c)** High magnification projected confocal images of the boxed region in (**a**). Filled arrowheads denote GFP^{+}NG2^{+}GFAP^{-} OPCs (O). **(d)** Representative GFP^{+} cells at 2 dpi include RGLs (R), astrocytes (A), and newborn intermediate neural progenitor cells (N) in Nf1^{Nestin} animals. **(e)** Quantification of total GFP^{+} cell numbers by lineage across the dentate gyrus at 2 dpi. Values represent mean ± s.e.m. Scale bars: 100 μm (**a**) and 10 μm (**c–d**). See Supplementary Table 1 for numbers of animals examined under different conditions.

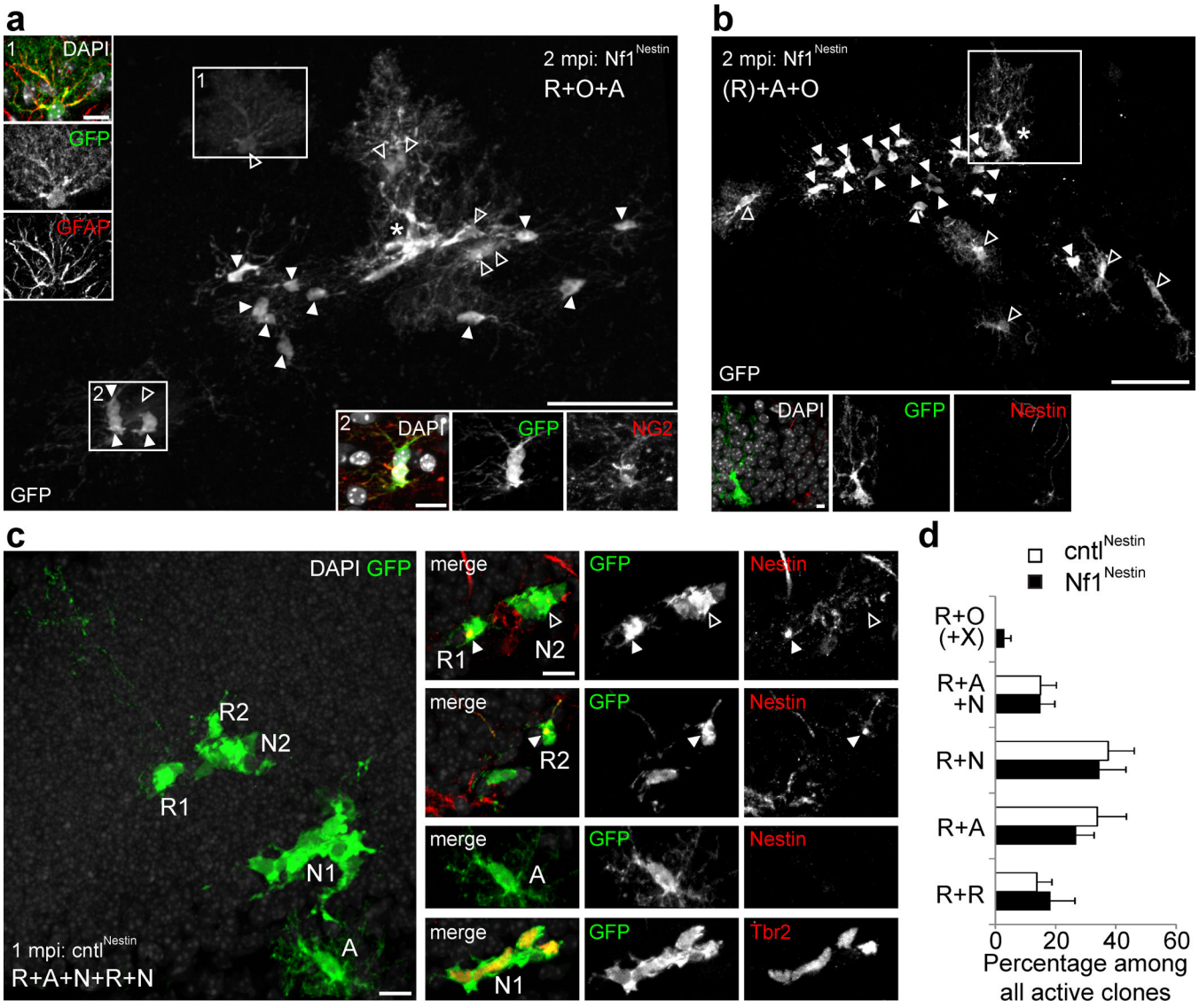

Figure 2.

Clonal lineage-tracing of RGLs upon conditional *Nf1* inactivation reveals RGLs as OPC cell of origin. **(a)** A clone at 2 mpi in $Nf1^{Nestin}$ animal with a maintained RGL (R: *), OPCs (O: filled arrowheads; See example in inset 2), and astrocytes (A: open arrowheads; See example in inset 1). Scale bars: 50 μm and 10 μm (inset). **(b)** A clone at 2 mpi in $Nf1^{Nestin}$ animal with differentiated RGL (*), OPCs (filled arrowheads), and astrocytes (open arrowheads). Inset: the differentiated RGL still possesses radial morphology but lacks expression of nestin. Scale bars: 50 μm and 10 μm (inset). **(c)** A clone at 1 mpi in $control^{Nestin}$ animal with maintained RGL (R1, R2) that underwent at least three rounds of division to symmetrically self-renew into two $nestin^{+}$ RGLs (R1, R2), generate two distinct clusters of $Tbr2^{+}$ newborn intermediate neural progenitor cells (N1, N2), and a $nestin^{-}$ astrocyte (A). Scale bar: 10 μm. **(d)** Quantitative comparison of the frequency of different RGL fate choices observed at 1

mpi. Values represent mean ± s.e.m. See Supplementary Table 2 for number of hemispheres examined under different conditions.